Narrow Band Total Absorber at Near-Infrared Wavelengths Using Monolayer Graphene and Sub-Wavelength Grating Based on Critical Coupling

Ali Akhavan, Saeed Abdolhosseini, Hassan Ghafoorifard, and Hamidreza Habibiyan

***Abstract*—Graphene has originally low absorption at telecommunication wavelengths. Therefore, it is necessary to overcome this hurdle to use graphene as an absorption media in many optoelectronic devices. In this paper, a narrow-bandwidth graphene-based total absorber is numerically and theoretically investigated. The proposed structure consists of a graphene sheet on a Si rectangular grating, which is placed on SiO_2 spacer backed with the gold substrate. Due to the absence of plasmonic response of graphene in near infrared wavelengths, the method of critical coupling with guided mode resonance is employed to realize highly efficient absorption of light in the graphene sheet. The simulation results show that the maximum magnitude of absorption reaches near 100% (43-fold enhancement compared to isolated monolayer graphene absorption of 2.3%). Also, based on calculated results, the absorption of the proposed structure can be controlled by altering the geometrical parameters and chemical potential of graphene. In particular, the absorption spectrum is modulated by the external gate voltage. Moreover, we find that the operating wavelength is adjusted flexibly by an incident source angle. As a result, the proposed absorber has high directivity and can act similar to an antenna. The control ability of total absorption in the proposed structure provides potential applications for the realization of ultra-compact and high-performance optoelectronic devices, such as sensors and narrow-band filters.**

***Index Terms*—Light absorption, monolayer graphene, nanoscale, near-infrared, sub-wavelength structure.**

I. Introduction

GRAPHENE, a two dimensional material with hexagonal lattice and one atom thickness, has generated a tremendous amount of research works due to its extraordinary mechanical, electronic and optical properties [1]–[3]. It was fabricated from graphite with mechanical exfoliation by Novoselov and his colleagues [4] while nowdays it can be fabricated by chemical vapor deposition (CVD). Its tunable conductivity from near to far-infrared regime and ultra high carrier mobility make graphene an appropriate material for various applications such as biosensors [5], [6], optical modulators [7]–[9], absorbers [10], [11] and photodetectors [12], [13].

In recent years, the absorption enhancements in graphene have drawn increasing attentions from researchers. To boost graphene absorption in wavelengths ranging from visible to far-infrared, various approaches have been presented. From mid to far-infrared, a strong plasmonic response with extreme field confinement appears in graphene and it behaves similar to Drude-type material [14], [15]. Thus, in this region, the total absorption has been achieved by shaping the graphene into disks [16] and micro-ribbons [17]. Also, plasmon modes can be excited by deposition of the unpatterned graphene on subwavelength metallic or dielectric grating [18], [19]. In addition, the wide-range tunability of absorption is another benefit of graphene absorbers in this region [15]. At shorter optical wavelengths (visible/near-infrared regime), the above mentioned absorbers are not applicable because strong plasmonic responses cannot be excited [20]. This is because the interband transition dominates over the intraband transition, therefore graphene acts as a lossy dielectric material [21]. Actually, the monolayer graphene absorptivity is expressed by $A = \pi\alpha \approx 2.3\%$ in which α is the fine structure constant [22].

Recently, the different approaches and methods have been proposed in the visible/near-infrared wavelengths. Cai *et al.* designed a graphene absorber, which has inspired a periodic pattern of metal-dielectric-metal metamaterial with a maximum absorption of about 37.5% for monolayer graphene [23]. Piper *et al.* demonstrated total absorption in monolayer graphene by using critical coupling, which is controlled by two dimensional (2D) photonic crystal resonance properties. The full-width at half-maximum (FWHM) has been reported close to 14 nm [24]. In other work, they achieved near-unity absorption at wavelength of 1.32 μm by employing critical coupling to degenerate resonances with opposite symmetry. The quality factor (Q) was reported 170 [25]. Hu *et al.* proposed a multilayer subwavelength grating structure to realize perfect absorption in undoped graphene strips. In their design, non-normal incidence light has been used. Meanwhile, the absorption extremely reduces when the incident angle increases [26]. Lu *et al.* theoretically and numerically demonstrated that the absorption could be enhanced 34.8-fold (∼80%) by the excitation of the Tamm plasmon polaritons mode, which highly confined in silica spacer [27].

Manuscript received May 11, 2018; revised August 27, 2018 and October 7, 2018; accepted October 11, 2018. Date of publication October 16, 2018; date of current version November 2, 2018. (*Corresponding author: Hamidreza Habibiyan.)*

A. Akhavan and H. Ghafoorifard are with the Department of Electrical Engineering, Amirkabir University of Technology, Tehran 15875-4413, Iran (e-mail: aliakhavan@aut.ac.ir; ghafoorifard@aut.ac.ir).

S. Abdolhosseini is with the School of Electrical and Computer Engineering, University College of Engineering, University of Tehran, Tehran 14395-515, Iran (e-mail: s.abdolhosseini@ut.ac.ir).

H. Habibiyan is with the Photonics Engineering Group, Amirkabir University of Technology, Tehran 15875-4413, Iran (e-mail: habibiyan@aut.ac.ir).

Color versions of one or more of the figures in this paper are available online at http://ieeexplore.ieee.org.

Digital Object Identifier 10.1109/JLT.2018.2876374

Fan *et al.* utilized the graphene sheet coupled with low index periodic structures to improve graphene absorptivity in the near-infrared, which shows 99.4% absorption and FWHM of 18 nm [28]. Furchi *et al.* designed integrating graphene with a Fabry-Pérot microcavity that leads to absorbing over 60% of light in graphene [29]. In spite of several graphene-based total absorber proposed in recent years, it seems that a realizable scheme is still needed, and the parameters attributed to the performance of these structures should be improved.

In this work, we both theoretically and numerically study a graphene-based total absorption structure consisting of monolayer graphene on a Si rectangular grating, which is placed on SiO_2 spacer backed with the gold substrate. The finite-difference time-domain (FDTD) [30] and the rigorous coupled-wave analysis (RCWA) [31] methods are used to calculate the absorption response of the structure. In addition, the coupled mode theory (CMT) is employed to analyze the condition of total absorption [32]. To get more insight into the physical concepts of the proposed structure, we give a brief review of the critical coupling and guided mode resonance concepts. The effects of geometrical parameters, the incident angle of light and chemical potential of graphene sheet are investigated in details to tune optical parameters of the total absorber such as the operating wavelength and the resonance peak.

II. The Proposed Structure, Numerical and Theoretical Model

Fig. 1 illustrates the sketch of the proposed absorber consisting of the graphene sheet deposited on rectangular silicon (Si) grating with permittivity of ε_1, under which SiO_2 layer with permittivity of ε_2 is used as a spacer. To prevent the transmission of incident light, the flat gold (Au) substrate is used under the SiO_2 spacer. The geometrical parameters are the period (Λ), the width (w), the height (h) of Si grating, the Si thickness (d) and SiO_2 spacer thickness (t). The dielectric permittivities ε_1 and ε_2 are taken to be 12.11 and 2.19, respectively [33]. In calculations, the frequency dependence of Au refractive index is exploited from Palik's handbook [33]. Based on random-phase approximation (RPA), the sheet conductivity of graphene $\sigma_g(\omega) = \sigma_{intra} + \sigma_{inter}$ includes the contributions of intraband and interband transitions, which are expressed as [34]:

$$\sigma_{intra} = \frac{i2e^2 k_B T}{\pi\hbar^2(\omega + i\tau^{-1})} \ln\left[2\cosh\left(\frac{\mu_c}{2k_B T}\right)\right], \quad (1)$$

$$\sigma_{inter} = \frac{e^2}{4\hbar}\left[\frac{1}{2} + \frac{1}{\pi}\arctan\left(\frac{\hbar\omega - 2\mu_c}{2k_B T}\right) - \frac{i}{2\pi}\ln\frac{(\hbar\omega + 2\mu_c)^2}{(\hbar\omega - 2\mu_c)^2 + 4(k_B T)^2}\right], \quad (2)$$

where $\hbar$ is the reduced Planck constant, e is the electron charge, k_B is the Boltzmann constant, T is the Kelvin temperature, ω is the angular frequency, μ_c is the chemical potential (Fermi energy) and $\tau = \mu\mu_c/ev_F^2$ is the electron-phonon relaxation time. Here, Fermi velocity and carrier mobility are set to $v_F \approx 10^6$ ms and $\mu = 10000$ cm^2/(V.s), respectively. Due to graphenes 2D nature, it can be considered an optically uni-axial anisotropic

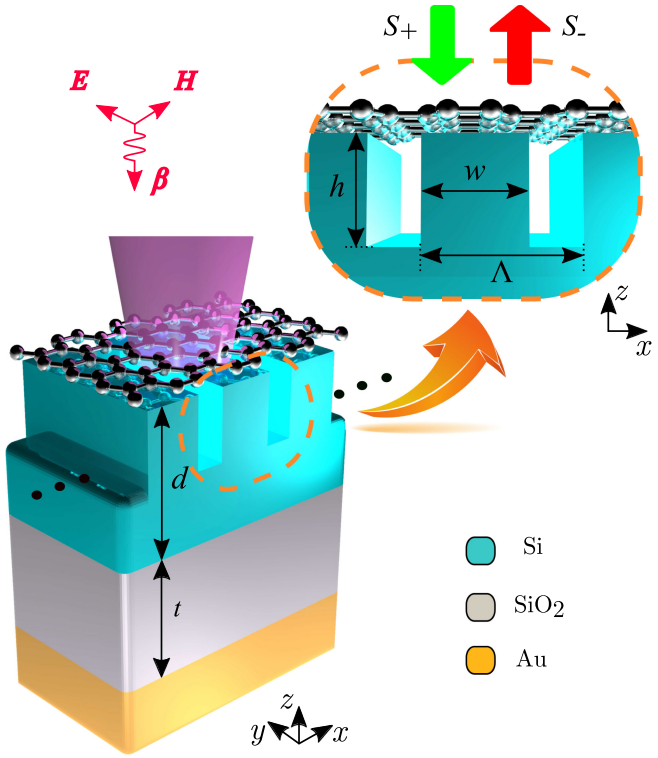

Fig. 1. Schematic diagram of the tunable graphene absorber under TE-polarized illumination. h stands for the Si grating height; d is the Si thickness and t is SiO_2 spacer thickness. Meanwhile, Λ and w represent Si grating period and width, respectively. Also, the cross sectional view of the periodic structure is indicated at the top of figure.

medium and its permittivity tensor in x-y plane can be written as [34]:

$$\varepsilon_g = \begin{bmatrix} \varepsilon_{g,\parallel} & 0 & 0 \\ 0 & \varepsilon_{g,\parallel} & 0 \\ 0 & 0 & \varepsilon_{g,\perp} \end{bmatrix}, \quad (3)$$

where $\varepsilon_{g,\parallel} = 2.5 + i\sigma(\omega)/\varepsilon_0\omega t_g$ and $\varepsilon_{g,\perp}$ is a constant value of 2.5. Here, ε_0 represents the vacuum permittivity and the graphene thickness t_g is approximately equal to 0.34 nm.

To realize total absorption in the proposed structure with the graphene sheet, the critical coupling condition should be satisfied. This occurs when the external leakage energy of a guided mode resonance is equal to intrinsic loss of the structure. In this condition, the incident light is totally coupled to guided mode resonance, which leads to enhance the power dissipation density around the graphene sheet. Consequently, significant enhancement is observed in absorption spectral features [24].

The proposed absorber is numerically simulated with FDTD method by setting periodic boundary conditions along the x-axis. Also, the perfectly matched layer (PML) is applied along the z-direction. To reduce simulation time and storage space, the non-uniform mesh is set and minimum mesh grid size inside the graphene sheet is equal to 0.034 nm. A transverse electric (TE)-polarized plane wave is normally incident on the structure in z direction. It should be noted that the source light is placed in the air with permittivity of $\varepsilon_a = 1$. The absorption spectrum

is defined as $A = 1 - T - R$ where R and T are reflectance and transmittance, respectively. However, in this paper, the value of T is near zero.

Since the width and height of the grating are smaller than the source wavelength, only the zero order guided resonance mode exists, which causes to appear one peak in the absorption spectrum. To get more insight into the critical coupling concept, the CMT is considered. The CMT describes input and output behavior of the resonator, which interferes coherently in the direct and indirect pathway. As can be seen in Fig. 1 , S_+ and S_- demonstrate the normalized input and output waves amplitudes, which pass through the port. At the single resonance frequency ω_0, the normalized amplitude of the guided resonance is a. γ_e denotes the external leakage rate. Actually, it depicts the time rate of the guided resonance amplitude variation of Si grating without the presence of input wave. By putting lossy material like graphene on Si grating, the dissipative losses in the guided resonance are described by intrinsic loss rate δ. With launching the incident light as a plane wave at frequency ω, the behavior of the system is expressed as below, based on time reversal symmetry and energy conservation [24]:

$$\frac{\mathrm{d}a}{\mathrm{d}t} = (j\omega_0 - \gamma_e - \delta)a + j\sqrt{2\gamma_e}S_+, \tag{4}$$

$$S_- = -S_+ - j\sqrt{2\gamma_e}a. \tag{5}$$

By using Eqs. (4) and (5), the reflection coefficient can be derived as:

$$r = \frac{S_-}{S_+} = -\frac{j(\omega - \omega_0) + \delta - \gamma_e}{j(\omega - \omega_0) + \delta + \gamma_e}, \tag{6}$$

and the absorbance of the system is:

$$A = \frac{4\delta\gamma_e}{(\omega - \omega_0)^2 + (\delta + \gamma_e)^2}. \tag{7}$$

From Eq. (7), to achieve total absorption of incident light at the resonance frequency $\omega = \omega_0$, the intrinsic loss of the system should be equal to the external leakage rate. In this condition, the critical coupling is realized.

III. Simulation Results and Discussions

The absorption spectra of the proposed structure under normal incidence with and without the monolayer graphene have been illustrated in Fig. 2 by using the FDTD method. As can be seen, the absorption spectrum is close to 5% when the graphene layer is removed. In other words, it comes from Au layer. However, in the presence of graphene, the total absorption is achieved. Geometrical parameters such as w, h, d, etc is optimized to achieve a total absorber. To this end, particle swarm optimization (PSO) is used to search the maximum absorbance by randomly selecting geometrical parameters [35]. By using the mentioned method, the optimal geometries are reached to enhance absorption of the monolayer graphene. The optimized parameters of the structure are chosen to be: $h = 130$ nm, $d = 270$ nm, $w = 510$ nm, $\Lambda = 530$ nm and $t = 300$ nm. Moreover, the chemical potential of graphene is set as 0.3 eV. It can be found that the maximum absorbance and FWHM are achieved 99.96 and 1.3 nm

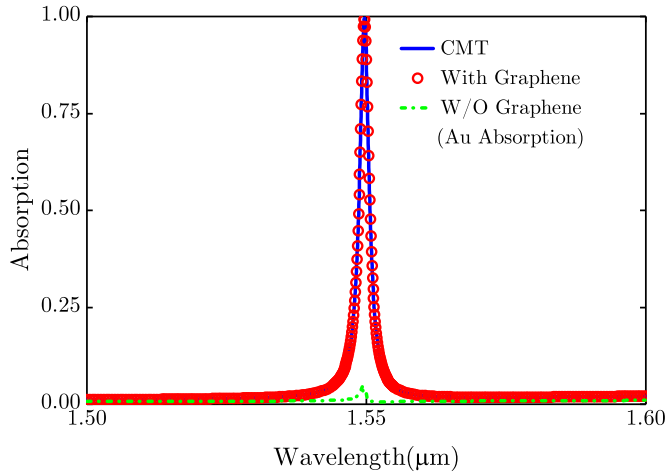

Fig. 2. FDTD Simulated absorption spectra of proposed structure in presence (red circle) and absence (green dash line) of monolayer graphene under normal incidence. Also, CMT-fitted absorption spectrum is plotted with blue solid line. The geometrical parameters are set as $h = 130$ nm, $d = 270$ nm, $w = 510$ nm, $\Lambda = 530$ nm and $t = 300$ nm. Moreover, the chemical potential is fixed $\mu_c = 0.3$ eV.

at the wavelength of 1550 nm, respectively. Consequently, the introduced device can widely be used as a total narrowband absorber. FWHM is an indication of the maximum allowable bandwidth of absorption. In other words, it is the shortest possible pulse-width in which the device can successfully support while maintaining its right operations. The appropriate FWHM (broader/narrower) depends on the application in which the total absorber is used. A larger FWHM leads to increase the bandwidth and hence the right operation can be applied on a shorter duration pulse which results to a high speed device. Thus, design of a broader FWHM is always desirable and is a crucial challenge in many applications such as high speed graphene based electro-absorption modulators [9]. However, in many other applications such as sensing, narrow-band absorption filters, etc, the narrower FWHM is preferable. When the suggested structure in Fig. 1 is surrounded by gas or liquid, a spectral shift in the absorption peak wavelength of Fig. 2 can be occurred due to the change of refractive index of environment. The ability to detect a variation in refractive index induced by trace amounts of analytes is limited by the line-width of the absorption spectrum. A narrower FWHM leads to detect a small shift in absorption peak that improves the sensor performance. Thus, in practical applications, narrow-band absorbers are often used as sensors [36].

The absorption spectrum, which is obtained from CMT, is observed in Fig. 2. It is clear that there is good agreement between CMT and FDTD results, especially at the resonant wavelength.

To better understand of the graphene's effect on absorbance and display how the light is dissipated in graphene on resonance wavelength, the power dissipation density is introduced as [21]:

$$w(x,z) = 0.5\varepsilon_0\omega\mathrm{Im}(\varepsilon(x,z))\left|E(x,z)\right|^2, \tag{8}$$

where $\varepsilon(x,z)$ stands for the permittivity of the constituent material of the structure. The electric field distribution and power

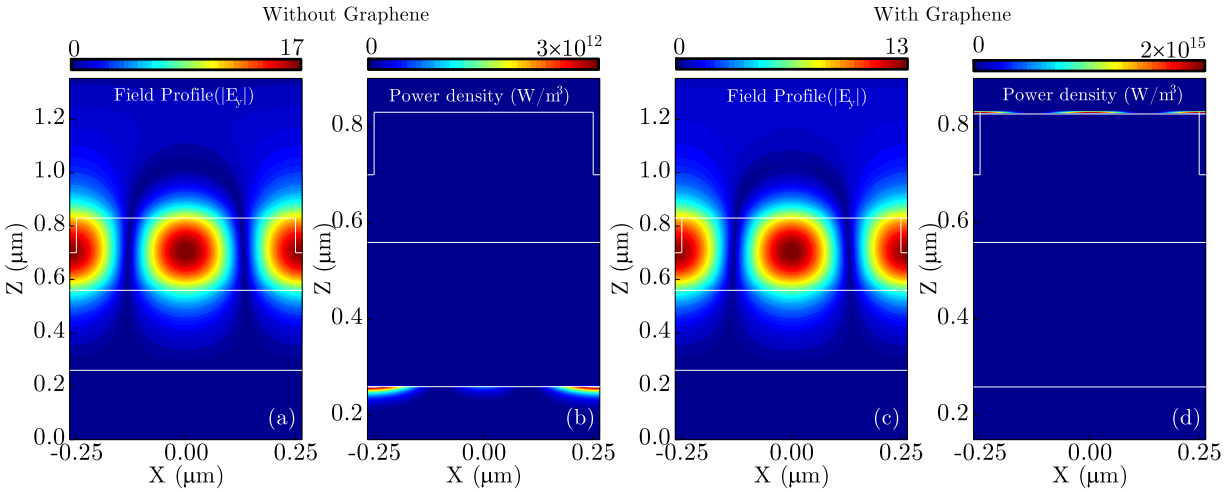

Fig. 3. (a) Electric field intensity of the structure and (b) power dissipation density (W/m^3) in absence of graphene at the wavelength of 1550 nm, (c) electric field intensity of the structure and (d) power dissipation density (W/m^3) in presence of graphene at the same wavelength.

dissipation density in presence and absence of graphene are demonstrated in Fig. 3. It can be clearly seen the electric field intensity for two cases is similar but the maximum magnitude of Fig. 3(a) is larger than Fig. 3(c). As shown in Fig. 3(c), at on-resonance mode, a large electric field is confined within Si grating, especially in the slit of air and middle of the grating. This phenomenon occurs due to the excitation of guided-mode resonances. In other words, the phase matching between the incident wave and guided mode resonance is satisfied by properly designing geometrical details of Si grating, which leads to exciting the guided mode resonance of Si grating. For more clarity and to justify why the difference of absorption between the two cases is so big, the power dissipation density is shown in Fig. 3(b) and Fig. 3(d). The presence of graphene causes near three order of magnitude enhancement in the power dissipation relative to absence of graphene. It shows that the graphene plays an important role to realize critical coupling and achieve total absorption.

As mentioned in Sec. II, δ and γ_e play a key role in realization of critical coupling. These parameters are directly related to geometrical parameters such as w, t and d. Therefore, it is expected that the absorption spectrum of the structure may be manipulated by variation of the Si grating width, SiO_2 spacer thickness and the Si thickness whereas other geometrical parameters remain unchanged. In the following, the effects of geometrical parameters of the structure are investigated.

A. *Effects of Geometrical Parameters on the Absorption Spectrum*

In the guided resonance system, γ_e is controlled by w. Hence, the absorption response can be tuned through critical coupling by adjusting w. The absorption spectra are demonstrated for different values of Si grating width (w) in Fig. 4(a). We have changed w in the range of 500 nm to 520 nm and other parameters are set at the same values mentioned before. As observed in Fig. 4(a), the absorption resonance wavelength shifts to the long wavelength as w increases. Meanwhile, the influence of w

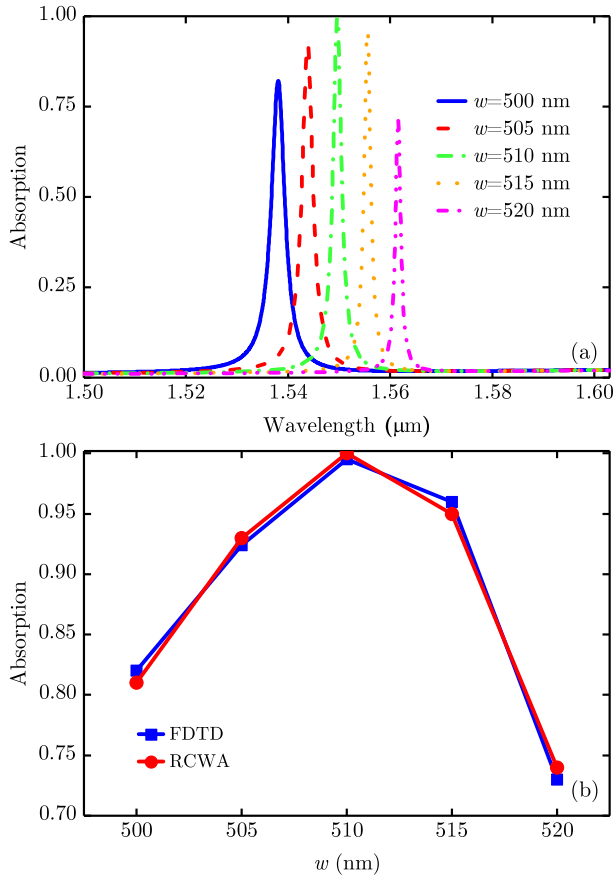

Fig. 4. (a) Absorption spectra of the proposed structure for different values of Si grating width (w) under normal incidence with TE-polarization. (b) Absorption resonance peak as a function of w. The other parameters are $h = 130$ nm, $d = 270$ nm, $\Lambda = 530$ nm, $t = 300$ nm and $\mu_c = 0.3$ eV.

variation in the absorption peak value is shown in Fig. 4(b). It is clear that by getting far from $w = 510$ nm, the peak value goes down. The results have been achieved by using RCWA and FDTD methods. It is clear that RCWA results have close agreement with FDTD simulation results.

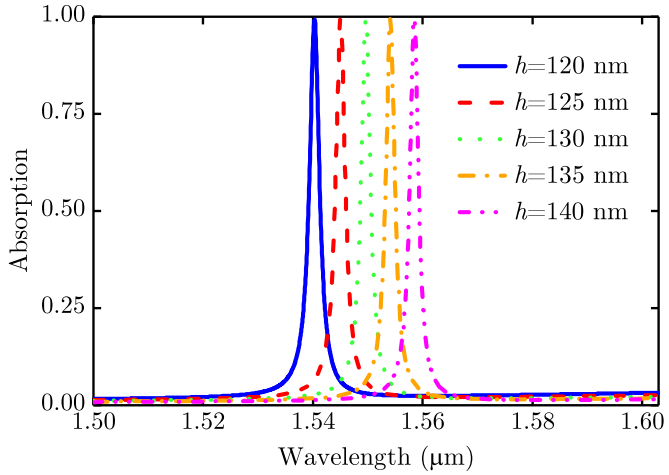

Fig. 5. Absorption spectra of the structure with various Si grating height, the remaining parameters are the same as those in Fig. 2.

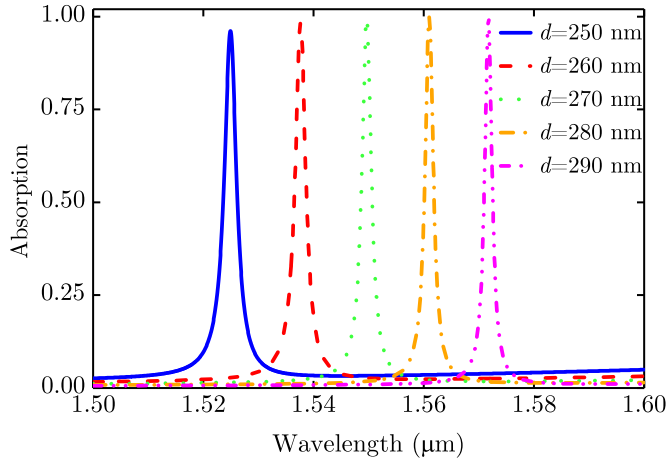

Fig. 6. Absorption spectra of the proposed structure for different values of Si thickness (d) under vertical illumination. Here, $h = 130$ nm, $w = 510$ nm, $\Lambda = 530$ nm, $t = 300$ nm and $\mu_c = 0.3$ eV.

By increasing the w, the leakage rate γ_e decreases while the intrinsic loss rate δ remains constant. Since FWHM is related to the sum of γ_e and δ, it decreases gradually. Also, the results exhibit the evolution of the system from overcoupling ($\gamma_e/\delta > 1$), through critical coupling, to the under coupling regime ($\gamma_e/\delta < 1$) [24].

In addition to Si grating width, the Si grating height will also affect the absorption characteristics of the periodic structure. Fig. 5 demonstrates absorption spectra dependence on the Si grating height (h) of the proposed structure under the normal incident light. The geometrical parameters are set similar to those used in Fig. 2. As shown in Fig. 5, the absorption resonance wavelength is pushed up when h is increased. In other words, by changing $\pm 8\%$ of h, the resonance wavelength can be tuned from 1540 nm to 1559 nm, which corresponds to the effective refractive index of the guided mode resonance. Unlike variations of resonance wavelength, the critical coupling can be maintained. Furthermore, the narrow FWHM for the absorption spectra is remained constant versus h alteration. Due to the high absorption capability of the proposed structure, the great error tolerance can be held against the fabrication process imperfections for Si grating height.

We proceed to study the influence of Si thickness (d) on the resonant characteristics of the proposed total absorber. The calculated absorption spectra are plotted in Fig. 6. When d increases, the absorption peak has a redshift. By variation of d from 250 nm to 290 nm, the resonance wavelength rises smoothly from 1525 nm to 1572 nm. In these simulations, the remaining parameters are set to $h = 130$ nm, $w = 510$ nm, $\Lambda = 530$ nm, $t = 300$ nm and $\mu_c = 0.3$ eV. The results indicate that absorption peak increases slightly with the increment of d. However, altering Si thickness has a negligible effect on FWHM of the absorption spectrum.

B. Role of Incident Angle on Optical Absorption

Up to now, the characteristics of the optical absorber have been investigated at normal incidence. Since the proposed absorber consists of grating configuration, we are interested to study its angular behavior. For this reason, a polar plot of the absorption at wavelengths of $\lambda_1 = 1550$ nm, $\lambda_2 = 1540$ nm and $\lambda_3 = 1500$ nm is shown in Fig. 7(a). As can be seen, their corresponding peak absorption are in the direction of 0°, 2.4° and 8°, respectively. Also, the peaks magnitude of absorption is calculated at 99.6, 98 and 92%, respectively. It is clear that by increasing the angle of incident, the absorption peak slightly decreases. The angular width at the three mentioned wavelengths is calculated at about 1.35°, 0.28° and 0.2°, respectively.

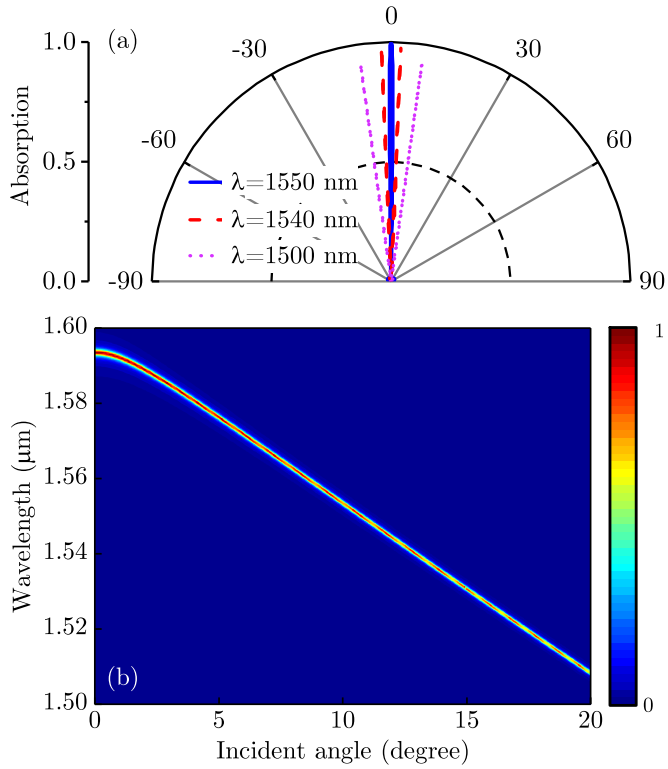

Fig. 7. (a) Absorption angular pattern at three operating wavelengths $\lambda = 1500, 1540, 1550$ nm. (b) Absorption map of the structure versus incident angle of light. The geometrical parameters are chosen $h = 130$ nm, $d = 270$ nm, $w = 510$ nm, $\Lambda = 530$ nm and $t = 300$ nm.

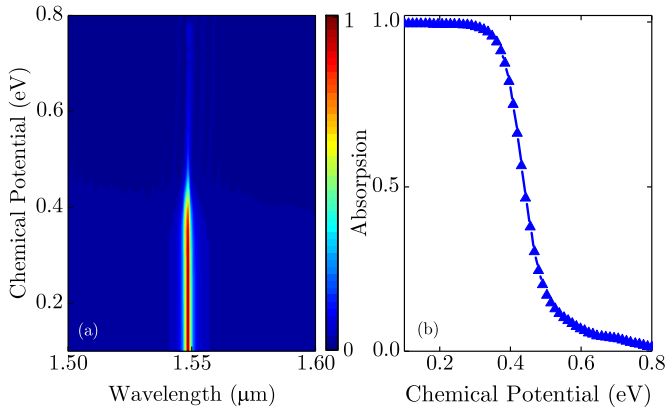

Fig. 8. (a) Absorption spectra of the proposed absorber versus chemical potential of monolayer graphene. (b) Variation of absorption resonance peak as a function of μ_c when the wavelength is 1550 nm.

Therefore, the angular width decreases when the incident wavelength is blue-shifted. Since the coherence length has an inversely proportional relationship with angular width, the decrement of angular width leads to improving spatial coherence. Therefore, the proposed absorber has high directivity and can act similar to an antenna. The absorption map as a function of incident angle and wavelength is demonstrated in Fig. 7(b). The map reveals that resonance wavelength blue shifts almost linearly with the incident angle variation. In addition, when the source is tilted, the absorption peak gradually decreases.

C. Tuning Absorption Response by the Chemical Potential of Monolayer Graphene

Finally, a brief investigation of the graphene chemical potential is presented. It is well known that the chemical potential of graphene can be controlled by external gate voltage [37]. In order to study the effect of chemical potential on absorption response of the structure, the contour map of the absorption versus wavelength and μ_c have been presented in Fig. 8(a). In the simulation, the geometrical parameters of the absorber are the same as those utilized in Fig. 2. Since the width of air grooves ($\Lambda - w = 20$ nm) is less than the Si grating ($w = 510$ nm), the inhomogeneous gating effect can be neglected and the surface conductivity of the whole graphene sheet can be considered homogenous [37]. As can be seen in Fig. 8(a), there is a rapid decrement of absorption around $\mu_c = 0.45$ eV. Particularly, at $\lambda = 1550$ nm, the absorption drops off from 0.93 to 0.11 when the chemical potential increases from 0.37 eV to 0.53 eV, as seen in Fig. 8(b). Actually, it can be realized that the monolayer graphene transfers from a lossy material to the lossless material by increasing the chemical potential near 0.45 eV. In other words, as μ_c is more than 0.45 eV, the critical coupling condition ($\gamma_e = \delta$) is not satisfied. Overall, applying external voltage provides a pathway to modulate absorption of the structure instead of variation of geometrical parameters.

In order to evaluate performance of the proposed structure, we compare our obtained results with other similar structures [24], [26], [28], [38]–[40]. Selected papers have been employed the critical coupling mechanism with guided resonances in telecommunication wavelengths. Table I shows the comparison between this work and the mentioned papers. It is obvious that the absorption resonance peak has been achieved close to 100% in all of them while the obtained FWHM are different. Therefore, in terms of FWHM, our introduced structure is more desirable for sensing applications and narrow-band absorption filters. In addition, the variation of absorption versus incident angle changes ($\Delta A/\Delta\theta$) has been studied. In our structure, as previously mentioned, by increasing the incident angle from 0° to 8°, the absorption peak decreases 8% and the value of ($\Delta A/\Delta\theta$) is calculated 0.95% per °. As can be seen in Table I, the obtained result for $\Delta A/\Delta\theta$ is less than other references. Therefore, the proposed structure shows better resistance to variation of incident angle. This feature makes it easy to use for realization of total absorption.

TABLE I
A COMPARISON OF PROPOSED ABSORBER WITH SIMILAR PLANS

References	Wavelength (nm)	Absorption (%)	FWHM (nm)	$\Delta A/\Delta\theta$ (% per °)
[24]	1500	100	14	1.13
[26]	1554	100	2.5	15.25
[28]	1526	99.4	18	–
[38]	1450	100	4	6
[39]	1612	100	2	6.6
[40]	1550	99	11	5
This work	1550	99.96	1.3	0.95

IV. CONCLUSION

In this paper, we proposed a new configuration of graphene-based total absorber. To reach the total absorption, the critical coupling with guided mode resonance mechanism was used in design of the structure. After optimization of suggested device using PSO method, the total absorption was achieved in the monolayer graphene at telecommunication wavelengths (near 100% of light at normal incident). Meanwhile, FWHM of 1.3 nm was obtained at a wavelength of 1550 nm. The simulation results have demonstrated that the absorption resonance peak and operating wavelength can be tuned by adjusting the chemical potential of the graphene sheet and the incident angle of light as well as the geometrical parameters. This tunable narrow-band absorber can be applied in design of graphene-based optoelectronic devices, sensors and narrow-band filters.

REFERENCES

[1] F. Bonaccorso, Z. Sun, T. Hasan, and A. C. Ferrari, "Graphene photonics and optoelectronics," *Nature Photon.*, vol. 4, no. 9, pp. 611–622, Sep. 2010.
[2] A. N. Grigorenko, M. Polini, and K. S. Novoselov, "Graphene plasmonics," *Nature Photon.*, vol. 6, no. 11, pp. 749–758, Jan. 2013.
[3] Q. Bao and K. P. Loh, "Graphene photonics, plasmonics, and broadband optoelectronic devices," *ACS Nano*, vol. 6, no. 5, pp. 3677–3694, May 2012.
[4] K. S. Novoselov *et al.*, "Electric field effect in atomically thin carbon films," *Science*, vol. 306, no. 5696, pp. 183–191, Oct. 2004.
[5] D. Rodrigo *et al.*, "Mid-infrared plasmonic biosensing with graphene," *Science*, vol. 349, no. 6244, pp. 165–168, Jul. 2015.

[6] Q. Li *et al.*, "Monolayer graphene sensing enabled by the strong Fano-resonant metasurface," *Nanoscale*, vol. 8, no. 39, pp. 17278–17284, 2016.
[7] M. Liu *et al.*, "A graphene-based broadband optical modulator," *Nature*, vol. 474, no. 7349, pp. 64–67, Jun. 2011.
[8] X. He, "Tunable terahertz graphene metamaterials," *Carbon*, vol. 82, no. C, pp. 229–237, Feb. 2015.
[9] Y. Hu *et al.*, "Broadband 10 Gb/s operation of graphene electro-absorption modulator on silicon," *Laser Photon. Rev.*, vol. 10, no. 2, pp. 307–316, Mar. 2016.
[10] P.-Y. Chen, M. Farhat, and H. Bac, "Graphene metascreen for designing compact infrared absorbers with enhanced bandwidth," *Nanotechnology*, vol. 26, no. 16, Apr. 2015, Art. no. 164002.
[11] R. Alaee, M. Farhat, C. Rockstuhl, and F. Lederer, "A perfect absorber made of a graphene micro-ribbon metamaterial." *Opt. Express*, vol. 20, no. 27, pp. 28017–28024, Dec. 2012.
[12] C.-H. Liu, Y.-C. Chang, T. B. Norris, and Z. Zhong, "Graphene photodetectors with ultra-broadband and high responsivity at room temperature," *Nature Nanotechnol.*, vol. 9, no. 4, pp. 273–278, Apr. 2014.
[13] J. Zhang, Z. Zhu, W. Liu, X. Yuan, and S. Qin, "Towards photodetection with high efficiency and tunable spectral selectivity: Graphene plasmonics for light trapping and absorption engineering," *Nanoscale*, vol. 7, no. 32, pp. 13530–13536, 2015.
[14] F. Wang *et al.*, "Gate-variable optical transitions in graphene," *Science*, vol. 320, no. 5873, pp. 206–209, Apr. 2008.
[15] F. H. L. Koppens, D. E. Chang, and F. J. García de Abajo, "Graphene plasmonics: A platform for strong light-matter interactions," *Nano Lett.*, vol. 11, no. 8, pp. 3370–3377, Aug. 2011.
[16] S. Thongrattanasiri, F. H. L. Koppens, and F. J. García de Abajo, "Complete optical absorption in periodically patterned graphene," *Phys. Rev. Lett.*, vol. 108, no. 4, Jan. 2012, Art. no. 047401.
[17] J. Christensen, A. Manjavacas, S. Thongrattanasiri, F. H. L. Koppens, and F. J. García de Abajo, "Graphene plasmon waveguiding and hybridization in individual and paired nanoribbons," *ACS Nano*, vol. 6, no. 1, pp. 431–440, Jan. 2012.
[18] W. Gao, J. Shu, C. Qiu, and Q. Xu, "Excitation of plasmonic waves in graphene by guided-mode resonances," *ACS Nano*, vol. 6, no. 9, pp. 7806–7813, Sep. 2012.
[19] T. R. Zhan, F. Y. Zhao, X. H. Hu, X. H. Liu, and J. Zi, "Band structure of plasmons and optical absorption enhancement in graphene on subwavelength dielectric gratings at infrared frequencies," *Phys. Rev. B*, vol. 86, no. 16, Oct. 2012, Art. no. 165416.
[20] Y. Liu *et al.*, "Approaching total absorption at near infrared in a large area monolayer graphene by critical coupling," *Appl. Phys. Lett.*, vol. 105, no. 18, Nov. 2014, Art. no. 181105.
[21] B. Zhao, J. M. Zhao, and Z. M. Zhang, "Resonance enhanced absorption in a graphene monolayer using deep metal gratings," *J. Opt. Soc. Amer. B*, vol. 32, no. 6, pp. 1176–1185, Jun. 2015.
[22] R. R. Nair *et al.*, "Fine structure constant defines visual transparency of graphene," *Science*, vol. 320, no. 5881, pp. 1308–1308, Jun. 2008.
[23] Y. Cai, J. Zhu, and Q. H. Liu, "Tunable enhanced optical absorption of graphene using plasmonic perfect absorbers," *Appl. Phys. Lett.*, vol. 106, no. 4, Jan. 2015, Art. no. 043105.
[24] J. R. Piper and S. Fan, "Total absorption in a graphene monolayer in the optical regime by critical coupling with a photonic crystal guided resonance," *ACS Photon.*, vol. 1, no. 4, pp. 347–353, Apr. 2014.
[25] J. R. Piper, V. Liu, and S. Fan, "Total absorption by degenerate critical coupling," *Appl. Phys. Lett.*, vol. 104, no. 25, Jun. 2014, Art. no. 251110.
[26] J.-H. Hu *et al.*, "Enhanced absorption of graphene strips with a multilayer subwavelength grating structure," *Appl. Phys. Lett.*, vol. 105, no. 22, Dec. 2014, Art. no. 221113.
[27] H. Lu, X. Gan, B. Jia, D. Mao, and J. Zhao, "Tunable high-efficiency light absorption of monolayer graphene via Tamm plasmon polaritons," *Opt. Lett.*, vol. 41, no. 20, pp. 4743–4746, Oct. 2016.
[28] Y. S. Fan *et al.*, "Monolayer-graphene-based perfect absorption structures in the near infrared," *Opt. Express*, vol. 25, no. 12, pp. 13079–13086, Jun. 2017.
[29] M. Furchi *et al.*, "Microcavity-integrated graphene photodetector," *Nano Lett.*, vol. 12, no. 6, pp. 2773–2777, Jun. 2012.
[30] A. Taflove and S. C. Hagness, *Computational Electrodynamics: The Finite-Difference Time-Domain Method*. Boston, MA, USA: Artech House, 2005.
[31] M. G. Moharam, T. K. Gaylord, E. B. Grann, and D. A. Pommet, "Formulation for stable and efficient implementation of the rigorous coupled-wave analysis of binary gratings," *J. Opt. Soc. Amer. A*, vol. 12, no. 5, pp. 1068–1076, May 1995.
[32] H. Haus and W. Huang, "Coupled-mode theory," *Proc. IEEE*, vol. 79, no. 10, pp. 1505–1518, Oct. 1991.
[33] E. Palik, *Handbook of Optical Constants of Solids*. San Diego, CA, USA: Academic, 1998.
[34] Y. Yao *et al.*, "Broad electrical tuning of graphene-loaded plasmonic antennas," *Nano Lett.*, vol. 13, no. 3, pp. 1257–1264, Mar. 2013.
[35] M. Shokooh-Saremi and R. Magnusson, "Particle swarm optimization and its application to the design of diffraction grating filters," *Opt. Lett.*, vol. 32, no. 8, pp. 894–896, Apr. 2007.
[36] D. Wu *et al.*, "Infrared perfect ultra-narrow band absorber as plasmonic sensor," *Nanoscale Res. Lett.*, vol. 11, no. 1, pp. 1–9, Dec. 2016, Art. no. 483.
[37] A. Vakil and N. Engheta, "Transformation optics using graphene," *Science*, vol. 332, no. 6035, pp. 1291–1294, Jun. 2011.
[38] G. Zheng, H. Zhang, and L. Bu, "Narrow-band enhanced absorption of monolayer graphene at near-infrared (NIR) sandwiched by dual gratings," *Plasmonics*, vol. 12, no. 2, pp. 271–276, Apr. 2017.
[39] J. Hu *et al.*, "Tailoring total absorption in a graphene monolayer covered subwavelength multilayer dielectric grating structure at near-infrared frequencies," *J. Opt. Soc. Amer. B*, vol. 34, no. 4, pp. 861–868, Apr. 2017.
[40] X. Jiang, T. Wang, S. Xiao, X. Yan, and L. Cheng, "Tunable ultra-high-efficiency light absorption of monolayer graphene using critical coupling with guided resonance," *Opt. Express*, vol. 25, no. 22, pp. 27028–27036, Oct. 2017.

Authors' biographies not available at the time of publication.